
Article:
Karaş, B., Smith, P.J., Fairclough, J.P.A. orcid.org/0000-0002-1675-5219 et al. (1 more author) (2022) Additive manufacturing of high density carbon fibre reinforced polymer composites. Additive Manufacturing, 58. 103044. ISSN 2214-8604

https://doi.org/10.1016/j.addma.2022.103044

Additive Manufacturing 58 (2022) 103044

Contents lists available at ScienceDirect

Additive Manufacturing

journal homepage: www.elsevier.com/locate/addma

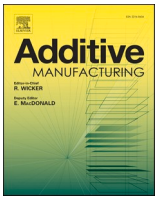

Additive manufacturing of high density carbon fibre reinforced polymer composites

Büşra Karaş *, Patrick J. Smith, J. Patrick A. Fairclough, Kamran Mumtaz

Mechanical Engineering Department, The University of Sheffield, Sheffield S1 4BJ, UK

ARTICLE INFO

Keywords:
Additive manufacturing
Sheet lamination
Carbon fibre reinforced polymer (CFRP) composites
Mechanical properties
X-ray computed tomography

ABSTRACT

Additive manufacturing (AM) of carbon fibre reinforced thermoplastic composites can offer advantages over traditional carbon fibre manufacturing through improved design freedom and reduction in production time and cost. However, the carbon fibre composites produced using current state-of-the-art AM approaches generally possess high porosity (18–25 %) compared to those produced by conventional manufacturing (1 %). An approach known as composite fibre additive manufacturing (CFAM) is presented, involving selectively printing a binder and polymer powder onto discontinuous carbon fibre sheets, which are then compressed, heated and post-processed to form net shape components. The results demonstrate a correlation between compaction pressure applied and porosity/fibre volume fraction within components. Composite components were produced containing porosity of 1.5 % and fibre volume content of 15 % with 97 MPa tensile strength and 8.9 GPa elastic modulus, presenting a new approach for production of discontinuous carbon fibre reinforced polymer parts with mechanical properties exceeding those of state-of-the-art AM.

1. Introduction

Carbon fibre reinforced polymer composites (CFRP) are used to create lightweight structures with high strength and stiffness. Using CFRP, it is possible to tailor mechanical properties specifically for an intended application by varying the volume of reinforcement and type of matrix material [1,2]. Thermosets and thermoplastics are two types of polymeric matrices. Thermosets are the conventionally preferred epoxy matrices used in the aerospace industry as they provide strong adhesion. However, thermoplastics usage is becoming popular due to their advantages in additive manufacturing (AM), such as melt processability and chemical resistance. The characteristics of thermoplastics decrease the complexity of curing cycles and make them more preferable for rapid manufacturing. Therefore, they can be easily processed using AM techniques [3]. AM of fibre reinforced thermoplastics is a major area of interest in academia and industry, as it presents an opportunity to combine the benefits of a composite's high strength to weight ratio with AM's design freedom to create functional, lightweight, complex geometries efficiently and cost-effectively [4].

Discontinuous or short fibres (a few millimeters in length) are currently more widely utilised in AM compared to continuous fibres. Discontinuous fibres are able to enhance the mechanical properties of the final parts without a significant modification to the overall manufacturing process. Hence, the integration of short fibres into standard feedstocks used in AM requires less resources, providing an advantage over continuous carbon fibre AM [5–7]. The addition of short fibre to polymer-based AM not only improves the strength and stiffness but also enables a flexible selection of matrix materials, which makes them more desirable in AM methods [3].

AM of fibre reinforced polymer composites can be processed through powder bed fusion, stereolithography, material extrusion and sheet lamination [8]. Powder bed AM processes such as Selective Laser Sintering (SLS) adopted discontinuous fibres within the polymeric matrices [9]. The mechanical properties of the final parts produced by the powder bed AM processes can be enhanced with the addition of short fibres, and there have been several studies reporting the mechanical improvements. Salazar et al. added short fibre glass (25 %wt) to the PA12 powder and produced composite parts that have 43.7 MPa tensile strength [10]. Similarly, CF/PA12 parts were fabricated via SLS and the tensile strength of the parts improved up to 66.7 MPa, showing 28 % increase compared to pure PA12 SLS parts. However the porosity of the CF filled parts found as 11–16 % in average, causing a significant reduce in elongation at break [11]. Jing et al. achieved 80 MPa tensile strength not only by combining CF with PA12, but also applying a surface

* Corresponding author.
E-mail address: bkaras1@sheffield.ac.uk (B. Karaş).

https://doi.org/10.1016/j.addma.2022.103044
Received 4 April 2022; Received in revised form 20 June 2022; Accepted 14 July 2022
Available online 16 July 2022

modification with nitric acid and heat treatment to the carbon fibres [12]. The porosity of the parts decreased from 38.12 % to 4.68 % as a result of the modification techniques, which is still a high amount of porosity compared to conventional composites [12].

As it is highlighted in the literature, the main disadvantages of composite SLS are the poor dispersion level of the fibre in the powder feedstock as well as the high level of internal porosity of the final composite parts [13]. It is also not possible to include continuous carbon fibres in the powder bed processes [13]. Although SLS is one of the fast growing AM technique for polymers and metals, there has been limited research on composites due to the limited mechanical property improvements at the cost of increases in component porosity [3].

Stereolithography (SLA) is another AM technique that adopts non-woven mats of carbon fibre, e-glass and para aramid fibres to produce composite parts with epoxy based resins. The highest tensile strength and stiffness reported using this approach was 55.2 MPa and 2.85 GPa respectively for the e-glass fibre reinforced acrylic based resin (17 g per square fibre mat) [14]. Similar to the SLS processes, limited research has been carried out on SLA of composites. Non-uniform distribution of the fibres on the surface of resin, poor bonding and high volume fraction of voids between the layers due to the partial curing are the drawbacks of adopting fibres in the SLA technique. Heat treatment, as a post processing method, was found to improve the mechanical properties [8].

Material extrusion-based techniques, such as Fused Filament Fabrication (FFF), are the most widely methods used for the production of fibre reinforced thermoplastic components. Printing of short fibres requires almost no alteration in FDM printers, whereas continuous fibres need some modification. Therefore, short fibre filaments are accessible and printable with desktop 3D printers. Continuous fibre filaments have been introduced to AM with the technique that Markforged developed. Continuous carbon fibre is embedded in-situ during the filament feedstock extrusion process creating reinforced nylon parts with an average tensile strength of 464.5 MPa and 35.7 GPa stiffness (V_f = 34.5 %), which is the highest mechanical performance for an AM composite polymer process without application of post treatment [15]. However, the mechanical properties are still lower than that of traditional continuous fibre reinforced composites manufacturing (e.g compression moulding tensile strength 1500 MPa and stiffness 135 GPa) due to low fibre volume fraction ratio [15]. Discontinuity of fibres due to printing pattern can cause a premature tensile failure in some Markforged components.

High void content is common in FFF continuous fibre composites due to the occurrence of triangular gaps between the printed tracks [16]. Justo et al. [17] stated that the lack of compaction in the FFF process caused a 12 % porosity between layers in continuous carbon fibre reinforced PA (Nylon) composites manufactured using the Markforged approach. In the case of discontinuous fibre composites, the strength and stiffness of the parts are lower compared to that of the Markforged continuous fibre composites. Tekinalp et al. [18] observed that the percentage of void volume in FFF printed carbon fibre reinforced ABS parts were between 16 % and 27 % regardless of fibre content. As the fibre content increased, tensile strength of the parts increased from 35 MPa to 65 MPa. However, high fibre reinforcement loading can also result in nozzle clogging causing a build to fail. Zhang et al. [19] printed short carbon fibre reinforced ABS composites that possessed tensile strengths and stiffness of 13.74–39.05 MPa and 2.19–5.89 GPa respectively for different raster orientations. The parts possessed 4.18–8.54 % porosity levels. Blok et al. (2018) achieved 1.1 % porosity for the short fibre reinforced nylon composites due to low fibre volume fraction (V_f = 6 %), while 9 % porosity was found in the parts printed by continuous CFRP filaments (V_f = 27 %). It was stated that there is a trade-off in performance and processability in terms of selection of continuous or discontinuous fibres. As the performance of the parts increases with the length of the fibres, the processability of the material is reduced [7].

In sheet lamination method, parts are manufactured by bonding the sheets of material. Currently there is a laminated object manufacturing technique to produce fibre reinforced polymer composites called Selective Lamination Composite Object Manufacturing (SLCOM) by the Envision Tec company. This technique uses both additive and subtractive approaches. Fibre reinforced sheets are cut by using an ultrasonic blade cutter. Then, these sheets are stacked together to form a 3D object by applying heat and pressure [20]. Another sheet lamination technique developed by Impossible Objects known as Composite Based Additive Manufacturing (CBAM) does not require cutting. Inkjet printing is used to print a liquid binder on a carbon fibre substrate layer, followed by a deposition of thermoplastic powder on the substrate. Then, the excess dry powder is removed, leaving an adhered powder behind with the cross-section of the printed geometry. After a sufficient number of layer have been produced, a hot press is used to compress printed sheets together and melt the polymer layers together. Finally the excess region of substrate layers is removed using a sandblaster [21,22]. The company claims that the parts with CBAM can be up to 10 times stronger as compared with other parts made by FDM or other 3D printing processes, although there are yet any published research output to this claim.

AM of composites has many challenges, including the limited availability of materials and a high percentage of porosity in the final parts. AM composite parts currently possess lower strength and higher void content than parts manufactured with conventional methods due to a lack of layer-to-layer compaction. Traditional composite manufacturing techniques use autoclave machines or heated rollers to improve the consolidation of layers which, in turn, improves mechanical performance of components [23]. The effects of applied pressure on mechanical and microstructural properties of traditionally made composites are widely investigated in literature. It has been identified that there is a correlation between the amount of pressure applied and the void content. An increase in the amount of pressure resulted in lower porosity, which improved the strength and stiffness of the parts [24–27]. There is currently no useful pressure applied in AM of composite structures (e.g material extrusion and powder bed fusion processes [7]). Research shows that post-processing of FFF printed composites using a hot press can significantly improve the tensile and flexural properties of FFF composite parts by decreasing the void content [28]. He et al. (2020) applied heat and pressure treatment to the 3D printed continuous CF/PA6 composites and achieved to reduce the void content from 12 % to 6 %, which improved the flexural properties [28]. Mei et al., 2019 [29] was able to increase the tensile strength of the FFF composite parts by 24 % through the use of a hot press, causing a reduction in the void content. Ueda et al. (2020) used hot compaction during 3D printing of continuous CFRP, which reduced the void content and improved the tensile and flexural properties of final parts. The void fraction has been reduced from 10 % to 3 %, while the tensile strength improved 24 % with the use of hot compaction [30]. An impregnation and a powder compression post-curing methods were used in [31] and significant increase was obtained in tensile properties of 3D printed continuous fibre reinforced thermosetting epoxy resin parts due to the high fibre fraction of 48 %. Compression post-curing reduced the void fraction from 10 % to 2.5 % [31]. However, the application of high heat and pressure is not practical to preserve FFF component geometry [32], although for sheet lamination processes, it can potentially enhance the strength and stiffness of the discontinuous fibre reinforced polymer parts by consolidating the layers. This provides strong inter-laminar bonding, resulting in smaller air gaps. To date, there is yet an independent academic study which has been reported using this approach to produce components, or study the effects of processing conditions on the resultant part properties.

In this paper, discontinuous CFRP composite parts were manufactured using a custom built system at the University of Sheffield, described as composite fibre additive manufacturing (CFAM), this approach is based upon a sheet lamination technique similar to CBAM. The aim of this study is to benchmark the performance of composite parts made by CFAM for the first time with mechanical testing and X-ray

tomography, with the aim of understanding the effects of the amount of printed ink, compaction pressure/time on the density and properties of final components.

2. Materials and methods

2.1. Material

A carbon fibre surfacing veil, incorporating randomly distributed short carbon fibres approximately 25 mm in length is bonded into a polyester matrix, supplied by ACP Composites (Livermore, CA, USA). This fabric is suitable for use in a wet layup and hot press applications. A 0.12 mm thick surfacing veil with 16.95 gsm was selected for experiments. As a matrix material, virgin PA 2200 (polyamide-12) supplied by EOS Gmbh (Krailling, Germany) was used. This polymer powder has a melting point of 185 °C and average grain size of 56 μm. It is commonly used in AM powder bed LS. HP Instant Ink 67/305 (Hewlett-Packard, Inc., Palo Alto, CA, USA) was used to print on carbon fibre sheets before applying polymer.

2.2. Composite fibre additive manufacturing approach (CFAM)

Discontinuous carbon fibre reinforced thermoplastic composite parts were fabricated using a custom built CFAM system as The University of Sheffield. The processing steps are shown in Fig. 1. The carbon fibre sheets were cut to a size of 148 × 210 mm, these were then inserted into one of two printing system to assess effect of printing volume. These printing systems were a HP Deskjet Plus 4130 inkjet printer (Hewlett-Packard, USA) and a drop on demand inkjet printer JetLab IV (MicroFab Technologies Inc., USA) with variable dots per inch (DPI) settings (represented as Inkjet head in Fig. 1a). After the first 2D slice of the part was printed onto the fibre sheet, PA2200 nylon powder was spread out onto the printed area, resulting in a coating/sticking of powder over the printed area (see Fig. 1b). Mild level of suction over the surface as shown in Fig. 1c was used to remove the dry excess powder from the surface of the fibre sheet. After the last 2D slice of the design was printed and coated, a hot press machine was used to compress printed sheets, forming a compact part bonded with melted nylon powder (Fig. 1d). Three different pressure levels (0.3, 0.6 and 0.9 MPa) were applied. The hot press chamber was heated to 210 °C (30 degrees above the melting point) to ensure the complete melting of nylon powder. After 20 min of ramping up time, the sample was left under pressure with three different dwell times (0.5 h, 1 h and 2 h), followed by cooling to ambient conditions. All the samples were cooled down using a cooling rate of 1 °C to stabilise the crystallisation process. The compressed part was removed from the hot press when the temperature of 40 °C was reached. Finally, a sandblasting process with blast media of brown alumina with low metallic iron content (Guyson Saftigrit Brown, Guyson International Ltd., Skipton, UK), was used to remove the excess carbon fibre layers that were not printed/coated with nylon powder (Fig. 1e), resulting in a CFRP part with the desired geometry as shown in Fig. 1f. Fig. 2 shows an example of a complex shape that was manufactured using the CFAM process developed at The University of Sheffield.

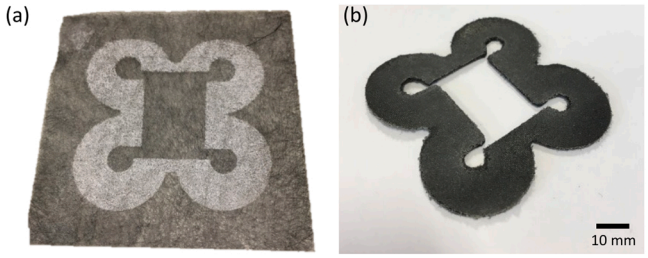

Fig. 2. Composite component made using the CFAM approach (a) printed layer before compression and bead blasting (b) final part with 24 layers.

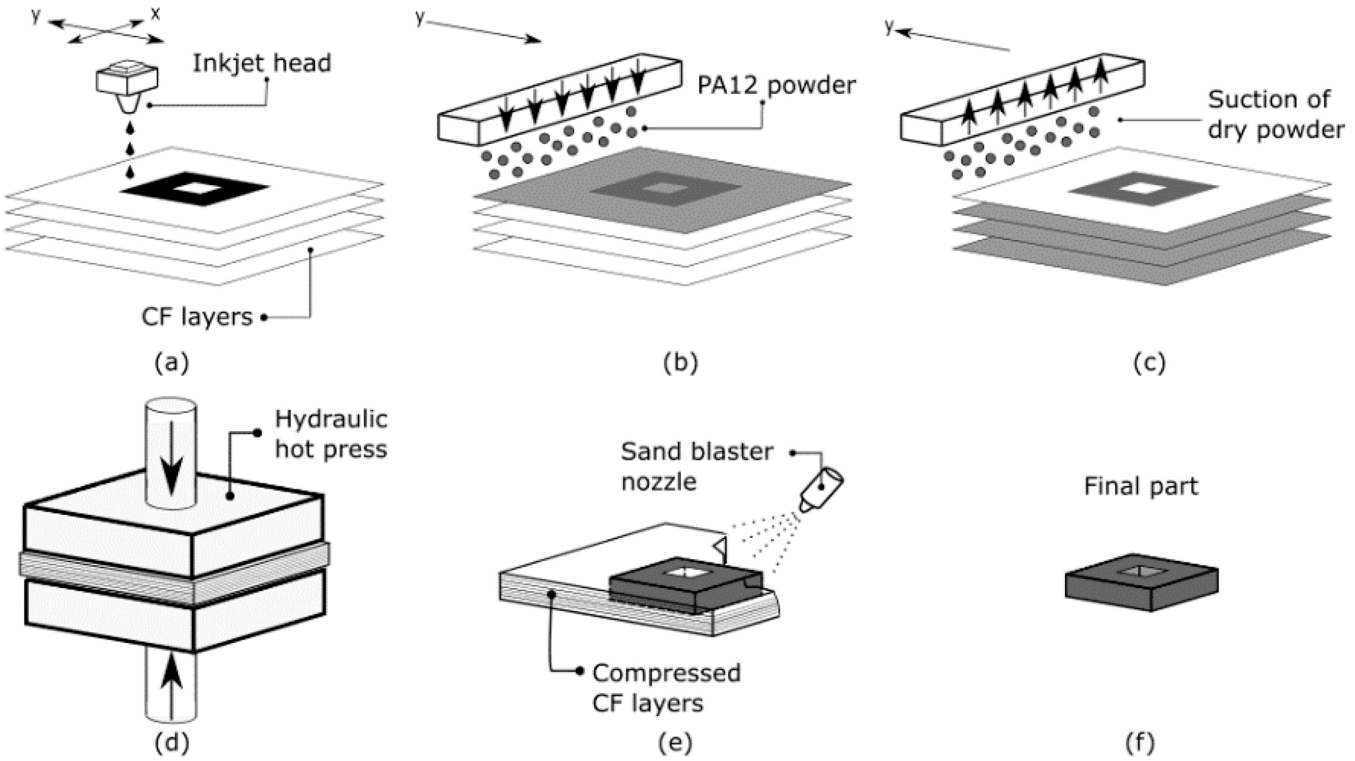

Fig. 1. Composite fibre additive manufacturing approach (CFAM); (a) inkjet printing, (b) deposition of polymer powder, (c) removal of excess dry powder, (d) hot press process, (e) removal of excess CF with sand blasting process, (f) final part.

2.3. Design of experiments

2.3.1. Process parameters

In traditional composite manufacturing, the effect of the autoclave process parameters on microstructural and mechanical properties of CFRP composites is widely investigated in literature. It has been observed that the optimum amount of pressure and vacuum application time decreased the void content significantly [24,26,33]. The hot press process provides the necessary pressure and heat to form a compact part within this technique, its processing parameters affect the final part properties. The ink volume determines the volume of powder that can be coated on a printed layer. The resolution of a desired geometry and adhesion of the layers can be affected by printing parameters. Based on these considerations, three factors were chosen: ink areal density, hot press pressure level and compaction time.

2.3.1.1. Ink areal density. The amount of ink per m^2 that is printed onto the carbon fibre sheet can be determined by the volume of the ink droplet ejected from the printhead. The volume of the ink droplet was 17.9 pL for HP Deskjet 4130, while it was 14 pL for the JetLab IV system. It is possible to adjust the droplet spacing and number of droplets in JetLab IV, while HP Deskjet printer has two automated high quality printing settings. Therefore, the low level of this factor has been obtained using JetLab IV. The amount of ink deposited with different dots per inch settings has been calculated as 24, 223 and 892 g/m^2 respectively by multiplying the volume of the ink droplet (μm^3) and DPI (dots per inch) setting of the printer.

2.3.1.2. Pressure level. The pressure is applied on the stacked carbon fibre layers to form a compact part bonded with melted nylon powder. Autoclave pressure between 0.3 and 0.6 MPa is generally used [24,34]. Factor levels were chosen as 0.3, 0.6 and 0.9 MPa. It has been observed that the final part width is expanded if a pressure higher than 0.9 MPa is applied due to squeezing the melted powder out of the printed region. Therefore, 0.9 MPa was the highest pressure level that can be applied.

2.3.1.3. Compaction time. The amount of time the part is kept under pressure during the dwell period. Factor levels were chosen as 0.5, 1 and 2 h.

Table 1 shows three process parameters with three levels as low, medium, and high levels.

2.3.2. Design of experiments using Taguchi analysis

The experiment aims to investigate the effect of process parameters on mechanical properties and porosity. A full factorial design would test all possible combinations. The Taguchi experimental design approach was used to determine the optimum parameter levels by testing a minimum number of combinations [35,36]. L9 orthogonal array was used as there are three factors with three different levels. Table 2 shows the experiment sets with the chosen parameter levels.

2.4. Measurements, characterisation and testing

2.4.1. Differential scanning calorimetry (DSC)

Differential scanning calorimeter (DSC) (Perkin Elmer DSC6) was used to investigate the thermal behaviour of nylon-12. The uncured samples of carbon fibre layers printed with nylon-12 weighing 1.2 mg was placed in a sealed DSC pan. The temperature was raised from 30 °C to 210 °C with a rate of 10 °C per minute, followed by 5 min hold at the maximum temperature. The cooling rate was 1 °C per minute back down to room temperature to represent the hot press cooling rate. The ramps were performed under a nitrogen purge of 50 mL/min.

Table 1
Process parameters with three levels.

Input parameter	Level-1	Level-2	Level-3
A = Pressure (Mpa)	0.3	0.6	0.9
B = Compaction time (hrs)	0.5	1	2
C = Ink areal density (g/m^2)	24	223	892

Table 2
Taguchi L9 orthogonal array for the design of experiments.

Experiment Set	Pressure (MPa)	Compaction time (h)	Ink areal density (g/m^2)
1	0.3	0.5	892
2	0.3	1	223
3	0.3	2	24
4	0.6	0.5	223
5	0.6	1	24
6	0.6	2	892
7	0.9	0.5	24
8	0.9	1	892
9	0.9	2	223

2.4.2. X-ray computed tomography (CT) scans and optical microscopy for porosity and fibre volume fraction analysis

The specimens for the tomography were manufactured as a cylinder geometry with 5 mm diameter and average thickness of 1 mm. They were scanned using the Zeiss Xradia Versa 620 X-ray Microscope (Pleasanton, Ca, USA). The scanning voltage was 70 kV with an X-ray source power of 8.5 W, and the current was 108 μA. Exposure time was 2.0 s per projection. A pixel size of 1.5 μm was obtained. The porosity and fibre volume fraction was calculated using the Dragonfly and FEI Avizo 9 software with segmentation by the Otsu method [37]. It is important to mention that the factors such as pixel size, magnification and subject contrast have an impact on the accuracy of the results. Therefore, following the pore and fibre segmentations, data statistics have been used to smooth the noise and refine the region of interest. These calculations were cross-checked by optical microscopy imaging using polished samples for each experimental set. Nicon Eclipse ME600 Metallurgical Microscope was used. Images were stitched to examine the maximum area. ImageJ software pack's FijiJ distribution was used for porosity and fibre volume fraction analysis.

2.4.3. Mechanical testing

Tensile specimens were manufactured as dog-bones according to the BS EN ISO 527–4:1997 Standards Type 1B specimen [38]. Fig. 3a shows the 2D slice of printed geometry on one carbon fibre substrate. To reach the average thickness of 2 mm, 40 layers of carbon fibre fabric were used and stacked layer by layer. 5 specimens for each experimental set were produced. Fig. 3b shows the compressed part after the hot press process, while Fig. 3c shows parts mid-way through sandblasting. Fig. 3d shows the final parts.

Tensile tests were performed utilising a Zwick tensometer 2020 Proline. Specimens were tested at a crosshead speed of 2 mm/minute. The flexural specimens, 5 repeats from each experimental set, were manufactured according to ASTM D7264 standard for three point bending test as 168 × 13×4 mm rectangles [39]. The thickness of the samples varied depending on the process parameters, however, the 32:1 support span- to-thickness ratio was kept constant. Flexural tests were performed using a Zwick tensometer 2020 Proline with a crosshead speed of 1 mm/minute.

3. Results

This section presents the variation of mechanical and porosity results of the samples in relation to fibre volume fraction and CFAM process parameter levels, i.e. pressure, compaction time and the ink areal density.

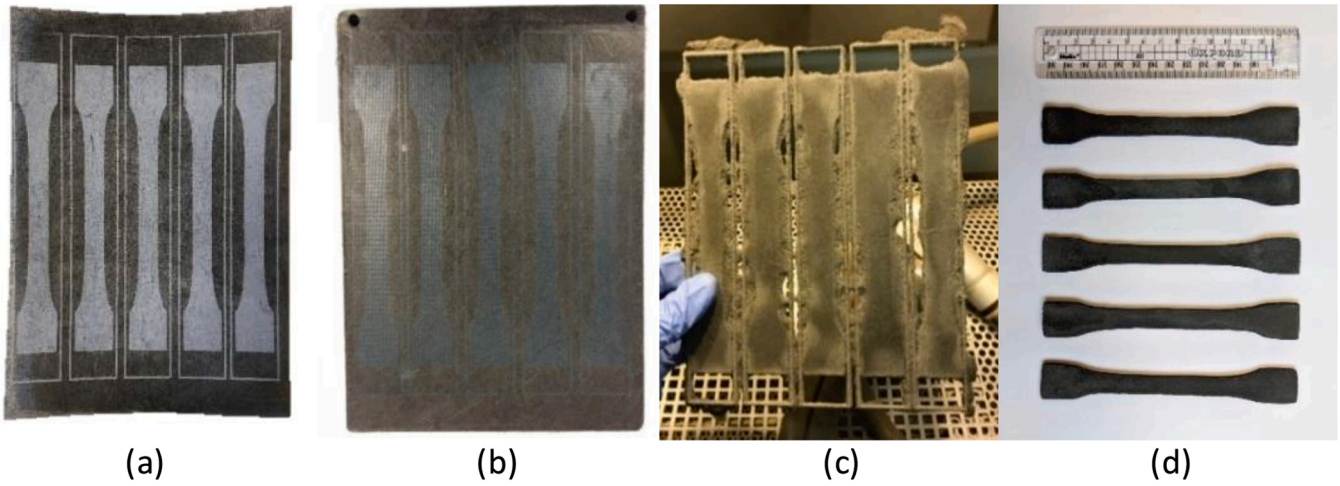

Fig. 3. Stages of CFAM manufacturing process (a) carbon fibre sheet after printing and deposition of powder; (b) stacked carbon fibre layers after hot press process; (c) sandblasting process mid-way through; (d) final dog bone samples.

3.1. DSC Analysis

DSC curve related to Nylon 12 (EOS Gmbh) is shown in Fig. 4. This experiment focused on the melting and crystallisation temperature of polymer powder in order to understand the appropriate duration for the samples to remain within the hot press. If the sample is removed early, carbon fibre layers will delaminate due to the polymer molecular chains not being able to diffuse a sufficient distance for them to work as a binder. The crystallisation temperature range of Nylon 12 was found to be 160–165 °C. Samples were heated up to 210 °C (30 °C more than the melting temperature) to ensure the powder was thoroughly melted through each layer. Samples were then removed after a set dwell time within the hot press after cooling down to 40 °C.

Table 3
Porosity and fibre volume fraction of the samples for each experiment set.

Experiment Set	Pressure (MPa)	Compaction Time (h)	Ink Areal Density (g/m^2)	Porosity (%)	FVF (%)
1	0.3	0.5	892	15	8.1
2	0.3	1	223	121	11
3	0.3	2	24	9.4	10.7
4	0.6	0.5	223	4.2	12.8
5	0.6	1	24	4.6	13.7
6	0.6	2	892	5.2	11.1
7	0.9	0.5	24	2.7	16.1
8	0.9	1	892	7.1	14.3
9	0.9	2	223	1.5	15.1

3.2. X-ray CT and optical microscopy

High-resolution X-ray tomography was performed in order to understand the volumetric content of the parts. A number of researchers have used this technique to successfully determine the porosity and fibre content in composites [40–43]. In alignment with the literature, percentages of porosity and carbon fibre volume fraction (FVF) calculated by the segmentation method for each sample are shown in Table 3. The calculations were consistent with the results obtained from optical microscopy. The fibre volume content increased as the pressure increased since a more compact part with lower thickness was formed with higher consolidation.

X-ray CT images from low, medium and high pressure levels are shown in Fig. 5. Images on the left side indicate the top view of the cylinder part, while the images on the right show the cross-sectional view. Layer by layer structures cannot be observed due to consolidation and random alignment of the fibres. It can be seen that large voids occurred due to low pressure applied to the component, while the size of the voids decreased with higher amount of applied pressure.

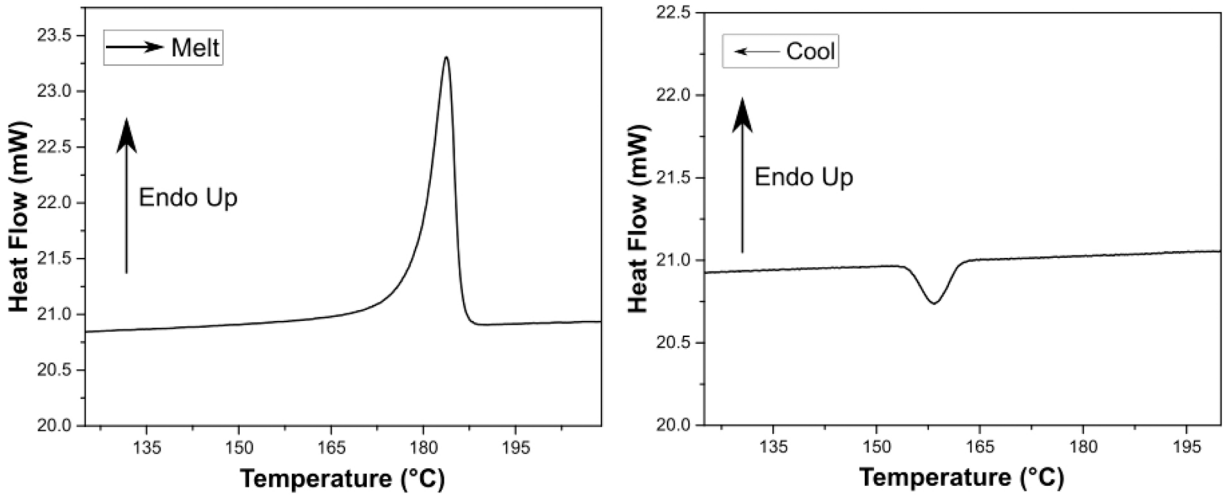

Fig. 4. DSC analysis of raw CF/Nylon-12 (1.2 mg) specimen.

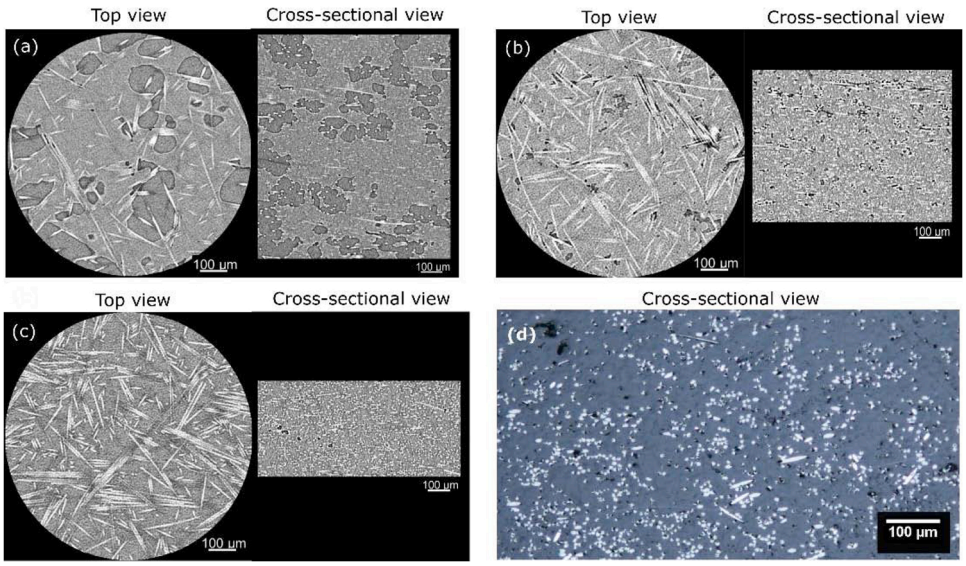

Fig. 5. X-ray CT images of different pressure settings; (a) Void content at low pressure level (0.3 MPa) (Set2) – Porosity: 12.1 %, (b) Void content at medium pressure level (0.6 MPa) (Set4)– Porosity: 4.2 %, (c) Void content at high pressure level (0.9 MPa) (Set9) – Porosity: 1.52 %, (d) Optical microscopy image for high pressure level (0.9 MPa) (Set 9) – Porosity: 1.59 %.

3.3. Mechanical testing

According to the tensile test results of the CFAM specimens, the maximum average tensile strength and stiffness was 97 MPa (± 1.8 %) and 8.9 GPa (± 1.5 %), respectively, for a sample that possessed a 15 % fibre volume fraction (Set 9). The maximum average flexural strength and stiffness were found to be 42.4 MPa (± 5 %) and 12.7 GPa (± 2 %), belonging to the same experimental condition (set 9). An improvement in both mechanical properties can be observed as the pressure increases from experimental set 1–2–3, to set 4–5–6 and finally to set 7–8–9. The difference between the sets using the same pressure level is not significant. However, this fluctuation increases as the pressure is set at the maximum level in sets 7, 8 and 9.

Taguchi design was analysed using Minitab 18 to determine the optimum parameter levels. Analysis of variance was undertaken using R software. Fig. 6 shows the main effects plots for tensile properties. The most significant factor that affects the tensile and flexural properties of the samples was found to be the amount of pressure with the lowest p-value (p = 4.85E-15). The highest level of pressure (0.9 MPa) gives the maximum tensile strength, elastic modulus, and flexural strength and modulus. The areal density of printed ink was the second significant factor. Medium parameter level, 223 g/m^2, ink was the optimum factor level generating the maximum output. Compaction time was found to be the least significant factor in this experiment.

It can be understood that pressure is the most influential factor. A considerable improvement can be observed as the pressure level increases in Fig. 7, showing the stress strain graphs for both tensile and flexural testing. Set 2,4 and 9 were chosen for comparison since they have the same parameter levels of compaction time and printed ink.

4. Discussion

The results indicate that the amount of pressure, compaction time, and the areal density of ink printed on the substrate within the CFAM process have a significant effect on the porosity content and carbon fibre volume fraction of short CFRP composites. As the amount of pressure and compaction time increases, the FVF of the samples also increases due to the reduced porosity within the sample, improving the mechanical properties. Flexural strength and stiffness were aligned with the tensile properties.

4.1. Effect of pressure on porosity and mechanical properties

Pressure is the most significant factor affecting the final part properties with the minimum p-value compared to other factors. The hjghest amount of pressure is preferred to improve both tensile and flexural properties. Since the layers are more compact, the thickness of the part is decreased, resulting in higher fibre volume fraction and lower porosity.

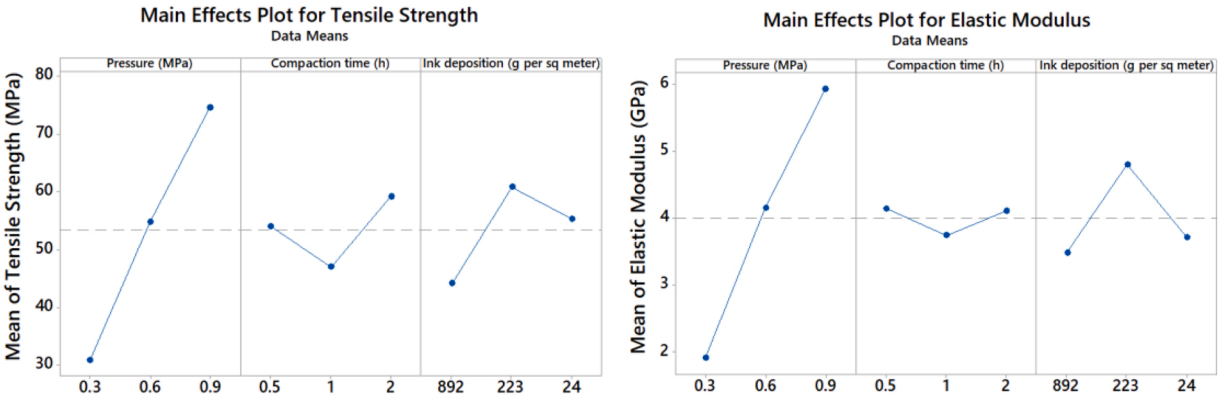

Fig. 6. Main effects plots for tensile strength and elastic modulus.

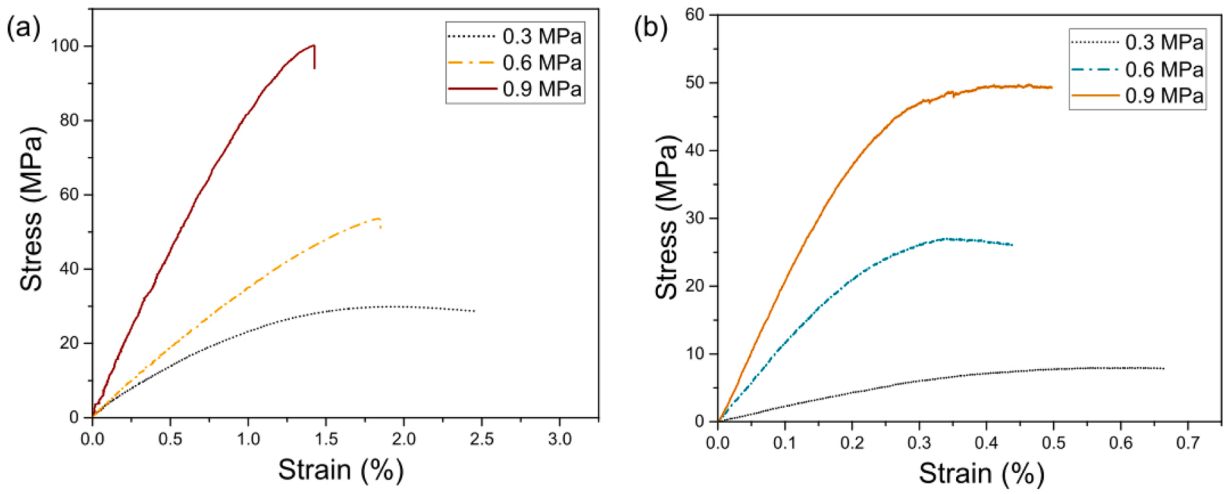

Fig. 7. (a) Tensile and (b) flexural test results for low, medium and high pressure levels.

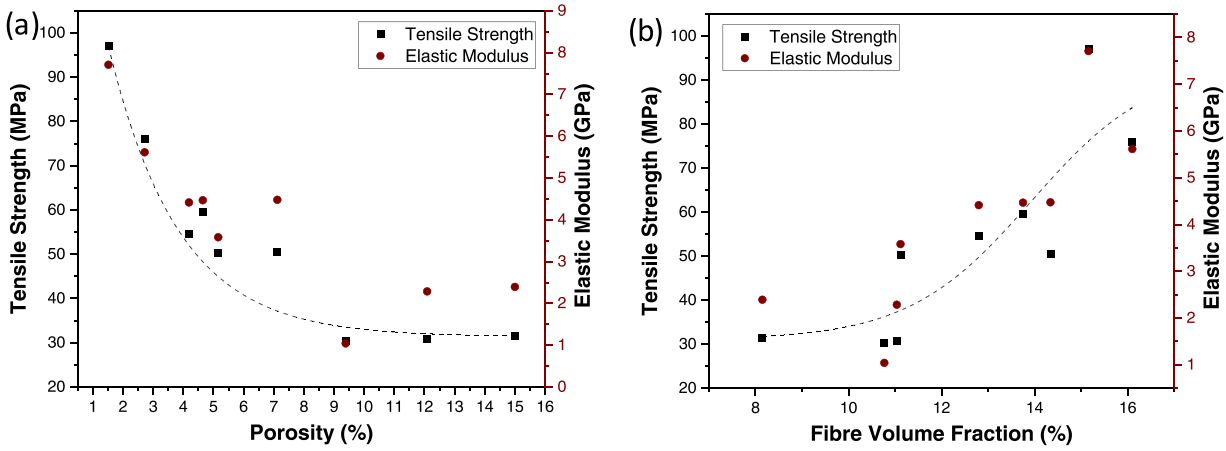

Fig. 8. (a) Relationship between porosity and tensile properties, (b) the relationship between fibre volume fraction and tensile properties.

Fig. 8 shows the relation between porosity and tensile properties, as well as the fibre volume fraction relationship. Each point represents a data set from the experimental design. As porosity increases, the tensile strength and elastic modulus of the parts decrease, presenting a strong correlation. One of the main disadvantages of composite AM approach is the void formation between the layers of the parts [44]. It was expected to have a high amount of void formation in this process since it has many factors which could result in the trapping of airinside of the thermoplastic powder and between layers. However, this study achieved 1.5 % porosity on average for the CFAM process ($Vf = 15$ %) with the optimum parameter levels due to the heat and pressure application.

4.2. Effect of ink areal density

It was observed that the areal density of ink printed per m^2 plays a vital role in the volume of powder that can be attached on the substrate, as a second significant factor after pressure. As the number of droplets increases, the amount of powder that can be used as a binding agent increases, resulting in a higher thickness of the final parts. This was verified by weighing the amount of powder for each level of ink. It has been found that 24, 223, 892 g/m^2 ink can accommodate 41.6, 208.3 and 291.6 g of powder per m^2 respectively. However, increase in the amount of binder due to higher number of droplets can also decrease the fibre volume fraction since the volume of the final part increases, but the number of carbon fibre fabric used in the reinforcement stays the same. Therefore, finding the optimal ink volume is essential to maximise the fibre volume fraction while providing a sufficient bonding between the carbon fibre fabric layers. Fig. 9 represents the amount of ink deposited per unit area (100 × 100 μm) for each printing setting, which is calculated based on the droplet size, dot-spacing and the number of ink droplets printed per unit area. It can be seen that low and medium printing settings have discrete droplets, while the printing with highest amount of ink per unit area creates overlapped droplets, therefore a complete layer.

The optimum parameter level for the maximum tensile strength and stiffness is 223 g/m^2 as this parameter level provides a strong fibre-matrix adhesion than the 24 g/m^2 of ink and a higher FVF than the 892 g/m^2 of ink. Samples printed with a low amount of ink showed low strength and stiffness despite the high fibre volume fraction due to the delamination failure that occurred in the early stage of mechanical testing. Fig. 10 shows the difference of failure between the samples printed with a low and medium amount of ink.

On the other hand, the highest amount of ink exhibits the highest amount of evaporation, since around 82.5 % of the ink is water. Non-uniform evaporation of the ink is likely to cause a high porosity level, as the amount of adhered powder is not distributed evenly.

Since HP Deskjet printer has two automated high-resolution printing settings, it is not possible to adjust the dot-spacing in between the values shown in Fig. 9b and c. JetLab IV printer can be used for this experiment, however, it is not practical to print larger geometries with a single nozzle, while the HP Deskjet printer has multiple nozzles that can print faster. Additionally, the optimal amount of ink found in this study shown

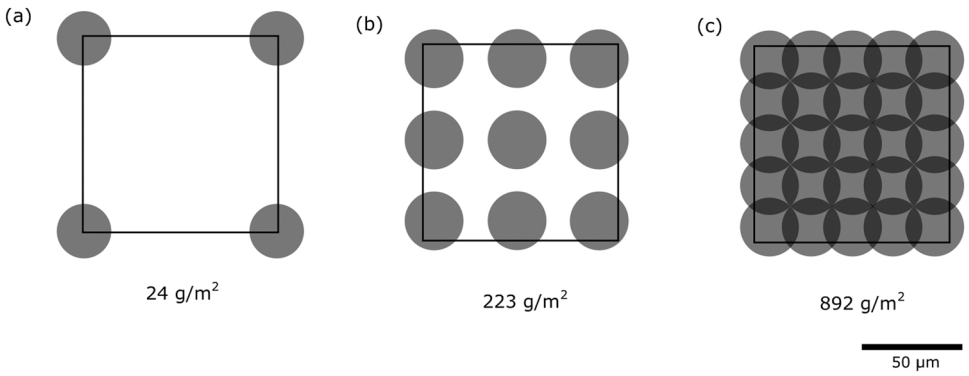

Fig. 9. Level of surface coverage for each printing setting; (a) 24 g/m^2 - JetLab IV, (b) 223 g/m^2 – HP Deskjet 600 DPI, (c) 892 g/m^2 – HP Deskjet 1200 DPI.

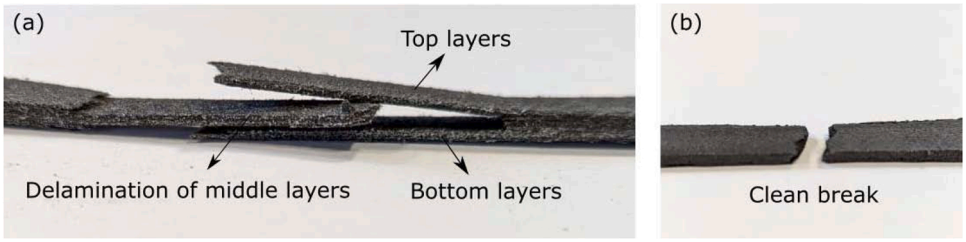

Fig. 10. Tensile failures of samples; (a) 24 g/m^2 ink, (b) 223 g/m^2 ink (0.3 MPa pressure and 2 h of compaction time kept constant).

in Fig. 9b can cover the interfaces of different powder particles (56 µm), which is sufficient to coat the whole surface of carbon fibre sheet with uniformly distributed powder.

4.3. Comparison with state-of-the-art

In general the performance of AM composites is low compared to traditional composite manufacturing [3,7]. High quality composites using traditional methods typically have a porosity content lower than 1 %, AM composite manufacturing techniques need to be improved in order to reach these densities. Reinforcing the polymers commonly used in AM with fibres can improve the mechanical properties but can also increase overall porosity within the component [45,46]. CFAM process achieves low porosity content of 1.5 % with 15 % fibre volume content. Compared with injection molding and LS of Nylon-12 parts with an average of 25 MPa and 40 MPa UTS respectively [47], the addition of fibres to the Nylon-12 in the CFAM process, increased the strength of the parts up to 97 MPa. This shows that fibres are effectively reinforcing the polymer matrix in CFAM process.

Fig. 11 shows the comparison of some of the reported mechanical properties for AM composites according to a review on AM of composites by Werken et al., (2020) [3]. It can be seen that CFAM parts produced parts with higher stiffness and tensile strength than additively manufactured discontinuous fibre composites but lower than continuous fibre composites (Markforged).

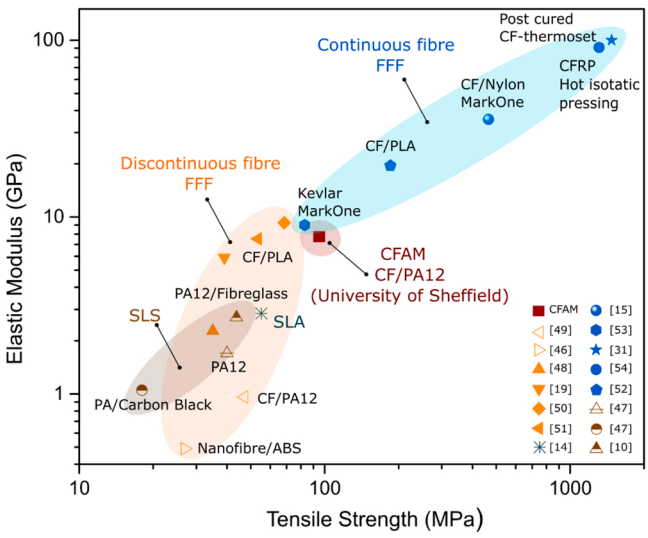

Fig. 11. Comparison between CFAM and other AM composite techniques with continuous and discontinuous fibre reinforcement [15,19,31,48–54].

5. Conclusions

The CFAM approach has demonstrated potential to form complex discontinuous fibre reinforced polymer composites parts with a higher strength, stiffness and density compared with state-of-the-art discontinuous fibre AM techniques (97 MPa tensile strength, 8.9 GPa stiffness and 1.5 % porosity). The technique may also offer the flexibility to process a variety of fibres (e.g glass fabrics with varying mesh density) and thermoplastic matrix materials (e.g. PEEK powder), further customising composite performance. The optimization of compaction time, ink areal density and pressure was shown to influence mechanical and microstructural properties of final CFAM parts. While compaction time has the lowest impact, the areal density of ink plays an important role on the amount of the polymer powder adhering to the substrate. It was observed that a low amount of ink increases the chance of interlayer delamination as there is no sufficient bonding between layers. However, as the volume of ink increases, the fibre volume fraction decreases due to a higher volume of matrix material. The use of elevated temperature and pressure facilitated the complete melting of nylon powder between layers, and reduced the component's overall porosity, this was shown to be the most significant factor affecting final part properties in terms of strength, stiffness and microstructural properties.

CRediT authorship contribution statement

Büşra Karaş: Writing – original draft, Visualization, Validation, Software, Resources, Methodology, Investigation, Formal analysis, Conceptualization. **Patrick J. Smith:** Writing – review & editing, Supervision, Resources, Methodology. **J. Patrick A. Fairclough:** Writing – review & editing, Supervision, Resources, Methodology. **Kamran Mumtaz:** Writing – review & editing, Supervision, Resources, Project administration, Methodology, Conceptualization.

Declaration of Competing Interest

The authors declare that they have no known competing financial interests or personal relationships that could have appeared to influence the work reported in this paper.

Data Availability

Data will be made available on request.

Acknowledgements

B. Karaş is grateful for the financial support from Turkish Ministry of Education. The authors gratefully acknowledge Sheffield Tomography Centre (STC), especially Ria L. Mitchell, at the University of Sheffield for their support and assistance.

References

[1] P.K. Mallick, Fiber-Reinforced Composites, CRC Press, 1946, CRC Press, 1946.
[2] J.R. Fekete, J.N. Hall, Design of auto body: materials perspective, Automot. Steels Des. Metall. Process. Appl. (2017) 1–18, https://doi.org/10.1016/B978-0-08-100638-2.00001-8.
[3] N. Van de Werken, H. Tekinalp, P. Khanbolouki, S. Ozcan, A. Williams, M. Tehrani, Additively manufactured carbon fiber-reinforced composites: state of the art and perspective, Addit. Manuf. 31 (2020), 100962, https://doi.org/10.1016/j.addma.2019.100962.
[4] F. Ning, W. Cong, Y. Hu, H. Wang, Additive manufacturing of carbon fiber-reinforced plastic composites using fused deposition modeling: effects of process parameters on tensile properties, J. Compos. Mater. (2017), https://doi.org/10.1177/0021998316646169.
[5] H. Yu, K.D. Potter, M.R. Wisnom, A novel manufacturing method for aligned discontinuous fibre composites (High performance-discontinuous fibre method), Compos. Part A 65 (2014) 175–185, https://doi.org/10.1016/j.compositesa.2014.06.005.
[6] M. Hashimoto, T. Okabe, T. Sasayama, H. Matsutani, M. Nishikawa, Composites: part A prediction of tensile strength of discontinuous carbon fiber / polypropylene composite with fiber orientation distribution, Compos. Part A 43 (2012) 1791–1799, https://doi.org/10.1016/j.compositesa.2012.05.006.
[7] L.G. Blok, M.L. Longana, H. Yu, B.K.S. Woods, An investigation into 3D printing of fibre reinforced thermoplastic composites, Addit. Manuf. 22 (2018) 176–186, https://doi.org/10.1016/j.addma.2018.04.039.
[8] D. Zindani, K. Kumar, An insight into additive manufacturing of fiber reinforced polymer composite, Int. J. Light. Mater. Manuf. 2 (2019) 267–278, https://doi.org/10.1016/j.ijlmm.2019.08.004.
[9] M. Chapiro, Current achievements and future outlook for composites in 3D printing, Reinf. Plast. (2016), https://doi.org/10.1016/j.repl.2016.10.002.
[10] A. Salazar, A. Rico, J. Rodríguez, J. Segurado Escudero, R. Seltzer, F. Martin De La Escalera Cutillas, Fatigue crack growth of SLS polyamide 12: effect of reinforcement and temperature, Compos. Part B Eng. 59 (2014) 285–292, https://doi.org/10.1016/j.compositesb.2013.12.017.
[11] A. Jansson, L. Pejryd, Characterisation of carbon fibre-reinforced polyamide manufactured by selective laser sintering, Addit. Manuf. 9 (2016) 7–13, https://doi.org/10.1016/j.addma.2015.12.003.
[12] W. Jing, C. Hui, W. Qiong, L. Hongbo, L. Zhanjun, Surface modification of carbon fibers and the selective laser sintering of modified carbon fiber/nylon 12 composite powder, Mater. Des. 116 (2017) 253–260, https://doi.org/10.1016/j.matdes.2016.12.037.
[13] G.D. Goh, Y.L. Yap, S. Agarwala, W.Y. Yeong, Recent progress in additive manufacturing of fiber reinforced polymer composite, Adv. Mater. Technol. 4 (2019) 1–22, https://doi.org/10.1002/admt.201800271.
[14] D.E. Karalekas, Study of the mechanical properties of nonwoven fibre mat reinforced photopolymers used in rapid prototyping, Mater. Des. 24 (2003) 665–670, https://doi.org/10.1016/S0261-3069(03)00153-5.
[15] F. Der Klift, Van, M. Ueda, A. Todoroki, Y. Hirano, R. Matsuzaki, Y. Koga, 3D printing of continuous carbon fibre reinforced thermo-plastic (CFRTP) tensile test specimens, Open J. Compos. Mater. 06 (2016) 18–27, https://doi.org/10.4236/ojcm.2016.61003.
[16] M. Handwerker, J. Wellnitz, H. Marzbani, Review of mechanical properties of and optimisation methods for continuous fibre-reinforced thermoplastic parts manufactured by fused deposition modelling, Prog. Addit. Manuf. 6 (2021) 663–677, https://doi.org/10.1007/s40964-021-00187-1.
[17] J. Justo, L. Távara, L. García-Guzmán, F. París, Characterization of 3D printed long fibre reinforced composites, Compos. Struct. 185 (2018) 537–548, https://doi.org/10.1016/j.compstruct.2017.11.052.
[18] H.L. Tekinalp, V. Kunc, G.M. Velez-Garcia, C.E. Duty, L.J. Love, A.K. Naskar, C. A. Blue, S. Ozcan, Highly oriented carbon fiber-polymer composites via additive manufacturing, Compos. Sci. Technol. (2014), https://doi.org/10.1016/j.compscitech.2014.10.009.
[19] W. Zhang, C. Cotton, J. Sun, D. Heider, B. Gu, B. Sun, T.W. Chou, Interfacial bonding strength of short carbon fiber/acrylonitrile-butadiene-styrene composites fabricated by fused deposition modeling, Compos. Part B Eng. 137 (2018) 51–59, https://doi.org/10.1016/j.compositesb.2017.11.018.
[20] Selective Lamination Composites Object Manufacturing Available online: ⟨https://envisiontec.com/wp-content/uploads/2016/09/2017-SLCOM1.pdf⟩ (Accessed on Jan 27, 2022).
[21] Kaplan, L. CBAM: Composite Based Additive Manufacturing Available online: ⟨http://additivemanufacturingseries.com/wp-content/uploads/2017/04/Kaplan.pdf⟩.
[22] Swartz, R.; Gore, E.; Crist, B.; Bayldon, J.; Wagner, C.; Tarzian, N.; Su, E. WO2017139766 - Method and Apparatus for Automated Composite-Based Additive Manufacturing 2017.
[23] D.H.J.A. Lukaszewicz, C. Ward, K.D. Potter, The engineering aspects of automated prepreg layup: History, present and future, Compos. Part B Eng. 43 (2012) 997–1009, https://doi.org/10.1016/j.compositesb.2011.12.003.
[24] Sudarisman, I.J. Davies, Influence of compressive pressure, vacuum pressure, and holding temperature applied during autoclave curing on the microstructure of unidirectional CFRP composites, Adv. Mater. Res. 41–42 (2008) 323–328, https://doi.org/10.4028/www.scientific.net/amr.41-42.323.
[25] Y. Li, Q. Li, H. Ma, The voids formation mechanisms and their effects on the mechanical properties of flax fiber reinforced epoxy composites, Compos. Part A Appl. Sci. Manuf. 72 (2015) 40–48, https://doi.org/10.1016/j.compositesa.2015.01.029.
[26] V.M. Drakonakis, J.C. Seferis, C.C. Doumanidis, Curing pressure influence of out-of-autoclave processing on structural composites for commercial aviation, Adv. Mater. Sci. Eng. 2013 (2013), https://doi.org/10.1155/2013/356824.
[27] H. Zhu, B. Wu, D. Li, D. Zhang, Y. Chen, Influence of voids on the tensile performance of carbon/epoxy fabric laminates, J. Mater. Sci. Technol. 27 (2011) 69–73, https://doi.org/10.1016/S1005-0302(11)60028-5.
[28] Q. He, H. Wang, K. Fu, L. Ye, 3D printed continuous CF/PA6 composites: effect of microscopic voids on mechanical performance, Compos. Sci. Technol. 191 (2020), 108077, https://doi.org/10.1016/j.compscitech.2020.108077.
[29] H. Mei, Z. Ali, Y. Yan, I. Ali, L. Cheng, Influence of mixed isotropic fiber angles and hot press on the mechanical properties of 3D printed composites 27 (2019) 150–158, https://doi.org/10.1016/j.addma.2019.03.008.
[30] M. Ueda, S. Kishimoto, M. Yamawaki, R. Matsuzaki, A. Todoroki, Y. Hirano, A. Le Duigou, 3D compaction printing of a continuous carbon fiber reinforced thermoplastic, Compos. Part A Appl. Sci. Manuf. 137 (2020), 105985, https://doi.org/10.1016/j.compositesa.2020.105985.
[31] Y. Ming, Y. Duan, B. Wang, H. Xiao, X. Zhang, A novel route to fabricate high-performance 3D printed continuous fiber-reinforced thermosetting polymer composites, Materials 12 (2019), https://doi.org/10.3390/ma12091369.
[32] C. Pascual-gonzález, P.S. Martín, I. Lizarralde, A. Fernández, A. León, C.S. Lopes, Post-processing effects on microstructure, interlaminar and thermal properties of 3D printed continuous carbon fibre composites 210 (2021).
[33] H. Koushyar, S. Alavi-Soltani, B. Minaie, M. Violette, Effects of variation in autoclave pressure, temperature, and vacuum-application time on porosity and mechanical properties of a carbon fiber/epoxy composite, J. Compos. Mater. 46 (2012) 1985–2004, https://doi.org/10.1177/0021998311429618.
[34] A. Lystrap, T.L. Andersen, Autoclave consolidation of fibre composites with a high temperature thermoplastic matrix, J. Mater. Process. Technol. 300 (1998) 80–85, https://doi.org/10.1016/s0924-0136(97)00398-1.
[35] S. Maghsoodloo, S. Engineering, Strengths and limitations of Taguchi ' s contributions to quality, manufacturing, J. Manuf. Syst. 23 (2004) 73–126.
[36] N. Mohan, P. Senthil, S. Vinodh, N. Jayanth, A review on composite materials and process parameters optimisation for the fused deposition modelling process, Virtual Phys. Prototyp. (2017).
[37] N. Otsu, P.L. Smith, D.B. Reid, C. Environment, L. Palo, P. Alto, P.L. Smith, A threshold selection method from gray-level histograms, IEEE Trans. Syst. Man. Cybern. C (1979) 62–66.
[38] BS EN ISO Plastics — Determination of tensile properties. Part 1 Gen. Princ. 1997, doi:⟨10.1016/j.fertnstert.2015.12.022⟩.
[39] ASTM D7264/D7264M-07 Standard Test Method for Flexural Properties of Polymer Matrix Composite Materials. *Annu. B. ASTM Stand.* 2007, *i*, 1–11, doi: 10.1520/D7264.
[40] X.W. Yu, H. Wang, Z.W. Wang, Analysis of yarn fiber volume fraction in textile composites using scanning electron microscopy and X-ray micro-computed tomography, J. Reinf. Plast. Compos. 38 (2019) 199–210, https://doi.org/10.1177/0731684418811943.
[41] A. Morales-Rodríguez, P. Reynaud, G. Fantozzi, J. Adrien, E. Maire, Porosity analysis of long-fiber-reinforced ceramic matrix composites using X-ray tomography, Scr. Mater. 60 (2009) 388–390, https://doi.org/10.1016/j.scriptamat.2008.11.018.

[42] M.J. Emerson, K.M. Jespersen, A.B. Dahl, K. Conradsen, L.P. Mikkelsen, Individual fibre segmentation from 3D X-ray computed tomography for characterising the fibre orientation in unidirectional composite materials, Compos. Part A Appl. Sci. Manuf. 97 (2017) 83–92, https://doi.org/10.1016/j.compositesa.2016.12.028.
[43] P.A. Hessman, T. Riedel, F. Welschinger, K. Hornberger, T. Böhlke, Microstructural analysis of short glass fiber reinforced thermoplastics based on x-ray micro-computed tomography, Compos. Sci. Technol. 183 (2019), 107752, https://doi.org/10.1016/j.compscitech.2019.107752.
[44] T.D. Ngo, A. Kashani, G. Imbalzano, K.T.Q. Nguyen, D. Hui, Additive manufacturing (3D printing): a review of materials, methods, applications and challenges, Compos. Part B Eng. 143 (2018) 172–196, https://doi.org/10.1016/j.compositesb.2018.02.012.
[45] Love, L.J. Cincinnati Big Area Additive Manufacturing (BAAM). 2015.
[46] G. Liao, Z. Li, Y. Cheng, D. Xu, D. Zhu, S. Jiang, J. Guo, X. Chen, G. Xu, Y. Zhu, Properties of oriented carbon fiber/polyamide 12 composite parts fabricated by fused deposition modeling, Mater. Des. 139 (2018) 283–292, https://doi.org/10.1016/j.matdes.2017.11.027.
[47] S.R. Athreya, K. Kalaitzidou, S. Das, Mechanical and microstructural properties of Nylon-12/carbon black composites: Selective laser sintering versus melt compounding and injection molding, Compos. Sci. Technol. 71 (2011) 506–510, https://doi.org/10.1016/j.compscitech.2010.12.028.
[48] F. Ning, W. Cong, J. Qiu, J. Wei, S. Wang, Additive manufacturing of carbon fiber reinforced thermoplastic composites using fused deposition modeling, Compos. Part B Eng. 80 (2015) 369–378, https://doi.org/10.1016/J.COMPOSITESB.2015.06.013.
[49] M.L. Shofner, K. Lozano, F.J. Rodríguez-Macías, E.V. Barrera, Nanofiber-reinforced polymers prepared by fused deposition modeling, J. Appl. Polym. Sci. 89 (2003) 3081–3090, https://doi.org/10.1002/app.12496.
[50] D. Jiang, D.E. Smith, Anisotropic mechanical properties of oriented carbon fiber filled polymer composites produced with fused filament fabrication, Addit. Manuf. 18 (2017) 84–94, https://doi.org/10.1016/j.addma.2017.08.006.
[51] R.T.L. Ferreira, I.C. Amatte, T.A. Dutra, D. Bürger, Experimental characterization and micrography of 3D printed PLA and PLA reinforced with short carbon fibers, Compos. Part B Eng. 124 (2017) 88–100, https://doi.org/10.1016/j.compositesb.2017.05.013.
[52] R. Matsuzaki, M. Ueda, M. Namiki, T.K. Jeong, H. Asahara, K. Horiguchi, T. Nakamura, A. Todoroki, Y. Hirano, Three-dimensional printing of continuous-fiber composites by in-nozzle impregnation, Sci. Rep. (2016), https://doi.org/10.1038/srep23058.
[53] G.W. Melenka, B.K.O. Cheung, J.S. Schofield, M.R. Dawson, J.P. Carey, Evaluation and prediction of the tensile properties of continuous fiber-reinforced 3D printed structures, Compos. Struct. 153 (2016) 866–875, https://doi.org/10.1016/j.compstruct.2016.07.018.
[54] Van de Werken, N. Additively Manufactured Continuous Carbon Fiber Thermoplastic Composites for High-Performance Applications. 2019.